

# Efficient Solver for Mixed Finite Element Method and Control-Volume Mixed Finite Element Method in 3-D on Hexahedral Grids

J.D. Wilson<sup>a \*</sup>, R.L. Naff<sup>a</sup>, T.F. Russell<sup>b</sup>

<sup>a</sup>U.S. Geological Survey, Denver, CO USA

<sup>b</sup>University of Colorado at Denver, Denver, CO USA

An efficient solver for the mixed finite element (MFE) method on 3-D distorted hexahedral cells has been implemented. The method relies on being able to define a divergence-free subspace. The divergence-free subspace is used to eliminate the pressure variable from the set of equations, resulting in a symmetric positive definite system. The preconditioned conjugate gradient (PCG) method is used to solve the reduced system. A two-level additive Schwarz method is implemented as the preconditioner.

We show that the same efficient solver can be used for the control-volume mixed finite element (CVMFE) method. The CVMFE method uses a discontinuous vector test space which leads to more accurate velocities in the presence of discontinuous anisotropic hydraulic conductivities on distorted hexahedral grids.

## 1. INTRODUCTION

It has been shown that mixed methods [2] are desirable for simulation of flow in heterogeneous porous media. Mixed methods enforce continuity in the fluxes and therefore preserve mass locally. For the approximation of smooth functions on rectangular grids the lowest-order Raviart-Thomas mixed finite element (MFE) can exhibit superconvergence,  $O(h^2)$ , in the fluxes (integrated velocities) and the pressures [1]. To accurately model the geophysics of underground porous media a mapping of the grid to a non-orthogonal grid may be required. For non-smooth mappings and non-smooth coefficients the accuracy of the MFE method suffers. The control-volume mixed finite element (CVMFE) method can recover the optimal order of accuracy in a straightforward way with no additional complexities such as Lagrange multipliers [3,4].

A mixed method results in an indefinite system of equations. Standard iterative methods work best with a positive definite system. A positive definite system can be formed by introducing a divergence-free subspace and eliminating the pressure variable. The divergence-free subspace method has been implemented on tetrahedral grids [8] and on distorted hexahedral grids [9]. A discretization of a 3-D domain using distorted hexahedral cells allows for the modeling of complex hydrogeological systems with a minimum of unknowns. We demonstrate that the same procedure can be used for the CVMFE method.

---

\*Supported by the National Research Council Research Associateship Award

## 2. BASIC EQUATIONS

We consider, on a 3-D domain  $\Omega$ , a steady flow equation given by:

$$-\nabla \cdot \mathbf{K} \nabla p = f \quad \text{in } \Omega. \quad (1)$$

The symmetric positive definite tensor  $\mathbf{K}$  is the hydraulic conductivity,  $p$  is the hydraulic head, and  $f$  is a specific volumetric flow. A specific discharge  $\mathbf{v}$  is introduced using the Darcy relation:

$$\mathbf{v} = -\mathbf{K} \nabla p. \quad (2)$$

Equation (1) is then written as a system of first-order equations given by:

$$\mathbf{K}^{-1} \mathbf{v} + \nabla p = 0 \quad (3)$$

$$\nabla \cdot \mathbf{v} = f. \quad (4)$$

Boundary conditions on  $\partial\Omega = \partial\Omega_D \cup \partial\Omega_N$  are specified as:

$$p = q \text{ on } \partial\Omega_D \text{ and } \mathbf{v} \cdot \mathbf{n} = g \text{ on } \partial\Omega_N. \quad (5)$$

### 2.1. Mixed Finite Element Method

We multiply equations (3)-(4) by appropriate test functions and integrate by parts to get

$$\int_{\Omega} \mathbf{K}^{-1} \mathbf{v} \cdot \mathbf{w} \, d\Omega - \int_{\Omega} (\nabla \cdot \mathbf{w}) p \, d\Omega = - \int_{\partial\Omega_D} (\mathbf{w} \cdot \mathbf{n}) q \, d\partial\Omega \quad (6)$$

$$\int_{\Omega} (\nabla \cdot \mathbf{v}) \lambda \, d\Omega = \int_{\Omega} f \lambda \, d\Omega. \quad (7)$$

We wish to find  $\mathbf{v} \in \mathbf{V}$  and  $p \in \Lambda$  that satisfy (6)-(7) for all  $\mathbf{w} \in \mathbf{V}_0$  and all  $\lambda \in \Lambda$ . The spaces  $\mathbf{V}$ ,  $\mathbf{V}_0$ , and  $\Lambda$  are given by:

$$\begin{aligned} \mathbf{V} &= \{ \mathbf{v} \in (L^2(\Omega))^3 : \nabla \cdot \mathbf{v} \in L^2(\Omega), \mathbf{v} \cdot \mathbf{n} = g \text{ on } \partial\Omega_N \}, \\ \mathbf{V}_0 &= \{ \mathbf{v} \in (L^2(\Omega))^3 : \nabla \cdot \mathbf{v} \in L^2(\Omega), \mathbf{v} \cdot \mathbf{n} = 0 \text{ on } \partial\Omega_N \}, \\ \Lambda &= L^2(\Omega). \end{aligned} \quad (8)$$

We discretize equations (6)-(7) by introducing finite dimensional subspaces  $\mathbf{V}^h \subset \mathbf{V}$ ,  $\mathbf{V}_0^h \subset \mathbf{V}_0$ , and  $\Lambda^h \subset \Lambda$ . We want to find  $(\mathbf{v}^h, p^h) \in (\mathbf{V}^h \times \Lambda^h)$  such that

$$\begin{cases} a(\mathbf{v}^h, \mathbf{w}) - b(\mathbf{w}, p^h) = -G(\mathbf{w}), & \forall \mathbf{w} \in \mathbf{V}_0^h \\ b(\mathbf{v}^h, \lambda) = F(\lambda), & \forall \lambda \in \Lambda^h \end{cases} \quad (9)$$

where we use the more common bilinear and linear forms to represent the integrals in (6)-(7).

Let the divergence-free subspace,  $\mathbf{D}_0^h \subset \mathbf{V}_0^h$ , be given by:

$$\mathbf{D}_0^h = \{ \mathbf{w}^h \in \mathbf{V}_0^h : b(\mathbf{w}^h, \lambda) = 0, \quad \forall \lambda \in \Lambda^h \} \quad (10)$$

We write  $\mathbf{v}^h$  as a vector function  $\mathbf{v}_I^h \in \mathbf{V}^h$  plus a divergence-free correction as:

$$\mathbf{v}^h = \mathbf{v}_I^h + \mathbf{v}_D^h \quad (11)$$

where  $\mathbf{v}_I^h$  satisfies the second equation in problem (9) and  $\mathbf{v}_D^h \in \mathbf{D}_0^h$  satisfies

$$a(\mathbf{v}_D^h, \mathbf{w}) = -a(\mathbf{v}_I^h, \mathbf{w}) - G(\mathbf{w}), \quad \forall \mathbf{w} \in \mathbf{D}_0^h. \quad (12)$$

Neumann boundary conditions are incorporated into  $\mathbf{v}_I^h$ . Problem (12) is symmetric positive definite and has a unique solution. After solving for  $\mathbf{v}^h$  we retrieve the pressure,  $p^h$ , by solving the following well-posed problem:

$$b(\mathbf{w}, p^h) = a(\mathbf{v}^h, \mathbf{w}) + G(\mathbf{w}), \quad \forall \mathbf{w} \in \mathbf{V}_0^h. \quad (13)$$

### 3. DISCRETIZATION

To define the finite-dimensional subspaces we partition the 3-D domain  $\Omega = \cup Q_{i,j,k}$  into hexahedral elements [5,6]. Each hexahedral element  $Q_{i,j,k}$  is a trilinear image of the reference cube  $\hat{Q}$ . The trilinear mapping  $T_{i,j,k} : \hat{Q} \rightarrow Q_{i,j,k}$  associates any point  $\hat{\mathbf{r}} = (\hat{x}, \hat{y}, \hat{z})$  in  $\hat{Q}$  to the point  $\mathbf{r}_{i,j,k} = (x, y, z)$  in  $Q_{i,j,k}$ . The covariant vectors  $\mathbf{X}_{i,j,k}$ ,  $\mathbf{Y}_{j,k,i}$ , and  $\mathbf{Z}_{k,i,j}$  describe the geometry of  $Q_{i,j,k}$  and form the columns of the Jacobian matrix  $B_{i,j,k}$ . The volume Jacobian can be given by any one of the following equivalent equations:

$$J_{i,j,k} = \mathbf{X}_{i,j,k} \cdot (\mathbf{Y}_{j,k,i} \times \mathbf{Z}_{k,i,j}), \quad J_{j,k,i} = \mathbf{Y}_{j,k,i} \cdot (\mathbf{Z}_{k,i,j} \times \mathbf{X}_{i,j,k}), \quad J_{k,i,j} = \mathbf{Z}_{k,i,j} \cdot (\mathbf{X}_{i,j,k} \times \mathbf{Y}_{j,k,i}). \quad (14)$$

The discrete pressure space  $\Lambda^h$  is the space of piecewise constants with nodal values at the centers of the hexahedral cells. The discrete velocity space is constructed from lowest-order Raviart-Thomas vector functions defined on the reference cube and then mapped to the physical space via the Piola transformation [7,2]. The transformation of basis vector functions on the reference cube to two adjacent hexahedral cells defines a basis vector function in the physical space. These transformations and the set of vector functions that spans  $\mathbf{V}_0^h$  are given as:

$$\mathbf{v}_{i+1/2,j,k}^x = \begin{cases} (\hat{x}, 0, 0)^T & \rightarrow \hat{x} \mathbf{X}_{i,j,k} / J_{i,j,k}, & \text{on } Q_{i,j,k} \\ (1 - \hat{x}, 0, 0)^T & \rightarrow (1 - \hat{x}) \mathbf{X}_{i+1,j,k} / J_{i+1,j,k}, & \text{on } Q_{i+1,j,k} \end{cases} \quad (15)$$

$$\mathbf{v}_{j+1/2,k,i}^y = \begin{cases} (0, \hat{y}, 0)^T & \rightarrow \hat{y} \mathbf{Y}_{j,k,i} / J_{j,k,i}, & \text{on } Q_{i,j,k} \\ (0, 1 - \hat{y}, 0)^T & \rightarrow (1 - \hat{y}) \mathbf{Y}_{j+1,k,i} / J_{j+1,k,i}, & \text{on } Q_{i,j+1,k} \end{cases} \quad (16)$$

$$\mathbf{v}_{k+1/2,i,j}^z = \begin{cases} (0, 0, \hat{z})^T & \rightarrow \hat{z} \mathbf{Z}_{k,i,j} / J_{k,i,j}, & \text{on } Q_{i,j,k} \\ (0, 0, 1 - \hat{z})^T & \rightarrow (1 - \hat{z}) \mathbf{Z}_{k+1,i,j} / J_{k+1,i,j}, & \text{on } Q_{i,j,k+1} \end{cases} \quad (17)$$

Using the properties of the Piola transformation one can show, for example, that

$$b(\mathbf{v}_{i+1/2,j,k}^x, p^h) = \int_{Q_{i+1/2,j,k}} (\nabla \cdot \mathbf{v}_{i+1/2,j,k}^x) p^h \, dx dy dz = p_{i,j,k} - p_{i+1,j,k}. \quad (18)$$

This is how equation (13) can be solved.

The dimension of  $\mathbf{V}_0^h$  on a  $l \times m \times n$  grid (assuming pure Neumann boundary conditions) is  $(l-1)mn + l(m-1)n + lm(n-1)$ . The dimension of  $\mathbf{D}_0^h$  is less than the dimension of  $\mathbf{V}_0^h$  and can be computed as

$$\dim \mathbf{D}_0^h = \dim \mathbf{V}_0^h - \dim \Lambda^h. \quad (19)$$

A basis vector function in  $\mathbf{D}_0^h$  has its support on four elements and can be written in terms of a linear combination of basis vector functions in  $\mathbf{V}_0^h$ . The basis for  $\mathbf{D}_0^h$ , used in our implementation, is given as:

$$\mathbf{v}_{j+1/2,k+1/2,0}^x = \mathbf{v}_{j+1/2,k,0}^y - \mathbf{v}_{j+1/2,k+1,0}^y - \mathbf{v}_{k+1/2,0,j}^z + \mathbf{v}_{k+1/2,0,j+1}^z, \quad (20)$$

$$\mathbf{v}_{k+1/2,i+1/2,j}^y = \mathbf{v}_{k+1/2,i,j}^z - \mathbf{v}_{k+1/2,i+1,j}^z - \mathbf{v}_{i+1/2,j,k}^x + \mathbf{v}_{i+1/2,j,k+1}^x, \quad (21)$$

$$\mathbf{v}_{i+1/2,j+1/2,k}^z = \mathbf{v}_{i+1/2,j,k}^x - \mathbf{v}_{i+1/2,j+1,k}^x - \mathbf{v}_{j+1/2,k,i}^y + \mathbf{v}_{j+1/2,k,i+1}^y. \quad (22)$$

Note that in equation (20) we restrict the "x-slice" divergence-free basis functions to the single ( $i = 0$ ) "x-slice".

#### 4. CONTROL VOLUMES

The CVMFE method differs from the MFE method in that the test space consists of discontinuous vector functions. This eliminates the arbitrary restriction that the fluxes be continuous in the test space. We choose functions in the test space  $\mathbf{W}_0^h$  to satisfy a local Darcy equation on a control volume. Consider the following control volumes on the reference cube, where the characteristic function  $X_{i_S}$  describes the set  $S$ :

$$X_{i_{\hat{Q}_{-1/2,0,0}}} = \begin{cases} 1, & 0 \leq \hat{x} \leq 1/2 \\ 0, & \text{otherwise} \end{cases}, \quad X_{i_{\hat{Q}_{1/2,0,0}}} = \begin{cases} 1, & 1/2 \leq \hat{x} \leq 1 \\ 0, & \text{otherwise} \end{cases} \quad (23)$$

We define a control volume in the physical space by mapping the control volumes in (23) to two adjacent hexahedral cells via the trilinear mapping as follows:

$$Q_{i+1/4,j,k} = T_{i,j,k}(\hat{Q}_{1/2,0,0}), \quad Q_{i+3/4,j,k} = T_{i+1,j,k}(\hat{Q}_{-1/2,0,0}). \quad (24)$$

A control volume basis vector function defined on  $Q_{i+1/2,j,k} = Q_{i+1/4,j,k} \cup Q_{i+3/4,j,k}$  can thus be given as:

$$\mathbf{w}_{i+1/2,j,k}^x = \begin{cases} \mathbf{X}_{i,j,k}/J_{i,j,k}, & \text{on } Q_{i+1/4,j,k} \\ \mathbf{X}_{i+1,j,k}/J_{i+1,j,k}, & \text{on } Q_{i+3/4,j,k} \end{cases}. \quad (25)$$

In a similar manner we can define the control volumes  $Q_{i,j+1/2,k}$  and  $Q_{i,j,k+1/2}$ , and their corresponding control-volume test functions  $\mathbf{w}_{j+1/2,k,i}^y$  and  $\mathbf{w}_{k+1/2,i,j}^z$ .

Since  $\mathbf{W}_0^h$  is discontinuous, we need to define the divergence of a vector function in  $\mathbf{W}_0^h$  weakly and thus define the discrete  $b(\cdot, \cdot)$  bilinear form. Consider the vector function  $\mathbf{w}_{i+1/2,j,k}^x$  given by (25). Suppose we have a scalar function  $p \in H^1(\Omega)$ . We compute the following pretending in the first two equalities that  $\mathbf{w}_{i+1/2,j,k}^x$  is smooth:

$$\begin{aligned} b(\mathbf{w}_{i+1/2,j,k}^x, p) &= \int_{Q_{i+1/2,j,k}} (\nabla \cdot \mathbf{w}_{i+1/2,j,k}^x) p \, dx dy dz = - \int_{Q_{i+1/2,j,k}} \mathbf{w}_{i+1/2,j,k}^x \cdot \nabla p \, dx dy dz \\ &= \int_0^1 \int_0^1 \left[ (p_{\hat{x}=1/2})_{Q_{i+1/4,j,k}} - (p_{\hat{x}=1/2})_{Q_{i+3/4,j,k}} \right] d\hat{y} d\hat{z} \end{aligned}$$

To get the last equality we use  $\mathbf{X}_{i,j,k} \cdot \nabla p = \partial p / \partial \hat{x}$  and the continuity of the pressure across the face joining  $Q_{i+1/4,j,k}$  and  $Q_{i+3/4,j,k}$ . We use the approximation

$$\int_0^1 \int_0^1 \left[ (p_{\hat{x}=1/2})_{Q_{i+1/4,j,k}} - (p_{\hat{x}=1/2})_{Q_{i+3/4,j,k}} \right] d\hat{y} d\hat{z} \approx p_{i,j,k} - p_{i+1,j,k} \quad (26)$$

to define the  $b(\cdot, \cdot)$  bilinear form as:

$$b(\mathbf{w}_{i+1/2,j,k}, p) = p_{i,j,k} - p_{i+1,j,k} \quad (27)$$

which is the same definition we use for the MFE method. Using this definition for the  $b(\cdot, \cdot)$  bilinear form we can define the divergence-free vector test function subspace in exactly the same manner as for the MFE method. An efficient solver for the CVMFE method is completely analogous to the solver for the MFE method. The only possible difficulty is that the  $a(\cdot, \cdot)$  bilinear form is no longer symmetric in general. In the next section we will show that this is not a major problem as far as we have tested. The  $a(\cdot, \cdot)$  bilinear form is nearly symmetric and it is likely to be positive definite.

## 5. NUMERICAL RESULTS

We consider test problems where the exact solution is known. To measure the error in the velocities we use the following  $L^2$  norm

$$\|ev\| = \left( \sum_i Q_i [ev_i/A_i]^2 / \sum_i Q_i \right)^{1/2} \quad (28)$$

where for all faces  $F_i \in \Omega$ ,  $ev_i$  is the difference between the estimated and true fluxes,  $A_i$  is the area, and  $Q_i$  is the control volume straddling  $F_i$ . The  $L^2$  norm of the pressure error,  $\|ep\|$ , is measured using a midpoint rule. The pressures at these points tend to exhibit superconvergence and give better results than one would expect with a continuous  $L^2$  norm. This superconvergence has been observed in [1].

For each test problem we use a  $1/h \times 1/h \times 1/h$  grid where  $h = (1/2)^\alpha$ . We compute approximate solutions on grids for  $\alpha = 2, 3, 4, 5, 6$ . The PCG method is used to compute the approximate solutions. We iterate until the preconditioned residual is reduced by 5 orders of magnitude.

For the smaller test problems ( $\alpha = 2, 3$ ) we use a Cholesky factorization as the preconditioner, which is an exact inverse in the MFE method, but for the CVMFE method it is an approximate inverse when the grid is non-orthogonal and the matrix is non-symmetric. For  $\alpha = 4, 5, 6$  we use an overlapping additive Schwarz method where we compute the projection of the error onto subdomains and onto a coarse grid using the symmetric  $a(\cdot, \cdot)$  inner product defined for the MFE method.

Each of the test problems has a known true solution. The normal flux of the solution is always continuous and the pressure is also continuous. The boundary conditions can be chosen to be either flux or pressure. The additive constant in the pressure can be chosen arbitrarily as long as we keep the pressure continuous.

### 5.1. Test 1

The first experiment is to estimate uniform flow on a randomly distorted grid. The pressure is given by:

$$p = -x + b \quad (29)$$

The randomly distorted grid is assembled on a  $4 \times 4 \times 4$  grid and then uniformly refined in reference coordinates for the larger grids. The grid points can vary by as much as 10%

of the cell width from the orthogonal point. The main point of this exercise is to test the effectiveness of the MFE preconditioner when applied to the CVMFE method. In this test the CVMFE matrix is non-symmetric.

Table 1 shows that the efficient solver works equally well for either method. We see superconvergence for the pressure in both methods. The CVMFE method exhibits a slightly higher order of convergence for the velocities although the initial error is greater.

Table 1  
Accuracy of MFE and CVMFE methods for uniform flow on distorted grid.

1/h	MFE method			CVMFE method		
	iterations	$\ ev\ $	$\ ep\ $	iterations	$\ ev\ $	$\ ep\ $
4	1	3.162E-3	1.869E-3	5	1.180E-2	1.511E-3
8	1	9.874E-4	5.421E-4	5	3.210E-3	4.060E-4
16	16	3.061E-4	1.445E-4	16	8.815E-4	1.065E-4
32	16	9.903E-5	3.929E-5	16	2.391E-4	2.839E-5
64	16	3.404E-5	1.137E-5	17	6.432E-5	8.583E-6
		$O(h^{1.64})$	$O(h^{1.85})$		$O(h^{1.88})$	$O(h^{1.88})$

### 5.2. Test 2

The next experiment is from [1] where we have an orthogonal grid and a discontinuous coefficient. We solve the problem on the unit cube. The hydraulic conductivity and pressure are given by:

$$\mathbf{K} = \begin{cases} \mathbf{K}_1, & 0 < x < 0.5, \\ \mathbf{K}_2, & 0.5 < x < 1, \end{cases} \quad \mathbf{K}_1 = \begin{pmatrix} 14/9 & 7/9 & 0 \\ 7/9 & 2 & 0 \\ 0 & 0 & 2 \end{pmatrix}, \quad \mathbf{K}_2 = \begin{pmatrix} 1 & 1/2 & 0 \\ 1/2 & 2 & 0 \\ 0 & 0 & 2 \end{pmatrix}, \quad (30)$$

$$p = \begin{cases} -x^3 + b_1, & 0 < x < 0.5, \\ -\frac{7}{6}x^2 + b_2, & 0.5 < x < 1. \end{cases} \quad (31)$$

Table 2 shows that both methods exhibit the same order of convergence.

### 5.3. Test 3

The last test is from [3] where we have a discontinuous conductivity and a non-orthogonal grid. The test is a 2-D test, but it illustrates the advantage of using the CVMFE method. The domain is divided into three regions as shown in Figure 5.3. The conductivity and pressure in each region are given by:

$$\mathbf{K}_I = \begin{pmatrix} 1/4 & 1/4 & 0 \\ 1/4 & 4 & 0 \\ 0 & 0 & 1 \end{pmatrix}, \quad \mathbf{K}_{II} = \begin{pmatrix} 2 & 1 & 0 \\ 1 & 1 & 0 \\ 0 & 0 & 1 \end{pmatrix}, \quad \mathbf{K}_{III} = \begin{pmatrix} 2 & 1/2 & 0 \\ 1/2 & 1/2 & 0 \\ 0 & 0 & 1 \end{pmatrix}, \quad (32)$$

$$p_I = x^2 + b, \quad p_{II} = \frac{1}{16}y^2 + b, \quad p_{III} = \frac{1}{4}y^2 + b. \quad (33)$$

Table 2  
Accuracy of MFE and CVMFE methods for discontinuous conductivity.

1/h	MFE method			CVMFE method		
	iterations	$\ ev\ $	$\ ep\ $	iterations	$\ ev\ $	$\ ep\ $
4	1	1.302E-2	5.113E-3	1	1.285E-2	2.111E-3
8	1	3.198E-3	1.711E-3	1	3.186E-3	6.298E-4
16	17	7.958E-4	4.860E-4	18	7.945E-4	1.747E-4
32	18	1.989E-4	1.303E-4	18	1.991E-4	4.851E-5
64	18	5.172E-5	3.892E-5	18	5.184E-5	1.581E-5
		$O(h^{2.00})$	$O(h^{1.80})$		$O(h^{1.99})$	$O(h^{1.78})$

The results shown in Table 3 show that the MFE method has  $O(h)$  accuracy in the velocities while the CVMFE method has  $O(h^2)$  accuracy in the velocities. Both methods exhibit superconvergence in the pressure.

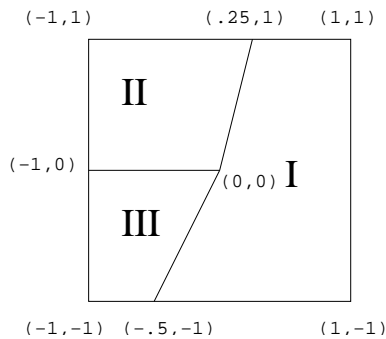


Figure 1. Distorted regions with variable conductivity.

## 6. CONCLUSIONS

We have shown that the efficient solver for the MFE method can be applied equally well to the CVMFE method. In cases where there is a variable conductivity tensor and a distorted grid the CVMFE method can give better approximations. We are also experimenting with transformations different from the Piola transformation that can recover some of the approximation properties in the velocities which can be lost on a distorted 3-D grid. In particular, one would expect the uniform flow problem in the first test to give exact solutions. It is shown in [6] why this is not so. We are also working on an efficient parallel solver using the message passing model. Initial prototypes of this parallel solver have produced good results.

Table 3  
Accuracy of MFE and CVMFE methods for discontinuous conductivity.

1/h	MFE method			CVMFE method		
	iterations	$\ ev\ $	$\ ep\ $	iterations	$\ ev\ $	$\ ep\ $
4	1	7.809E-3	1.564E-1	5	4.656E-3	1.030E-1
8	1	4.827E-3	4.168E-2	6	1.210E-3	2.747E-2
16	26	2.609E-3	1.071E-2	28	3.107E-4	7.070E-3
32	32	1.201E-3	2.698E-3	35	8.030E-5	1.776E-3
64	37	5.997E-4	6.806E-4	40	2.373E-5	4.609E-4
		$O(h^{0.99})$	$O(h^{1.96})$		$O(h^{1.91})$	$O(h^{1.96})$

## REFERENCES

1. T. Arbogast, P. T. Keenan, M. F. Wheeler, and I. Yotov. Logically rectangular mixed methods for Darcy flow on general geometry. In *Proceedings of the 13th SPE Symposium on Reservoir Simulation*, pages 51–59. Society for Petroleum Engineers, 1995.
2. F. Brezzi and M. Fortin. *Mixed and Hybrid Finite Element Methods*. Springer-Verlag, 1991.
3. Z. Cai, J.E. Jones, S.F. McCormick, and T.F. Russell. Control-volume mixed finite element methods. *Computational Geosciences*, (1):289–315, 1997.
4. V.A. Garanzha and V.N. Konshin. Approximation schemes and discrete well models for the numerical simulation of the 2-d non-Darcy fluid flows in porous media. Technical report, Russian Academy of Sciences Computer Centre, 1999.
5. T. Hughes. *The Finite Element Method*, pages 123–125. Prentice-Hall, Englewood Cliffs, N.J., 1987.
6. R. Naff, T. Russell, and J. Wilson. Test functions for three-dimensional control-volume finite-element methods on irregular grids. In Bentley, Sykes, Brebbia, Gray, and Pinder, editors, *Computational Methods in Water Resources*, volume 2, pages 677–684. Balkema, Brookfield, 2000.
7. P.A. Raviart and J.M. Thomas. A mixed finite element method for 2nd order elliptic problems. In I. Galligani and E. Magenes, editors, *Mathematical Aspects of Finite Element Methods, Lecture Notes in Mathematics*, volume 606, pages 292–315. Springer-Verlag, New York, 1977.
8. R. Scheichl. *Iterative Solution of Saddle Point Problems Using Divergence-free Finite Elements with Applications to Groundwater Flow*. PhD thesis, University of Bath, 2000.
9. J.D. Wilson. *Efficient Solver for Mixed and Control-Volume Mixed Finite Element Methods in Three Dimensions*. PhD thesis, University of Colorado at Denver, 2001.